

Sol-gel synthesis of monolithic molybdenum oxide aerogels and xerogels

Winy Dong and Bruce Dunn*

Department of Materials Science and Engineering, University of California, Los Angeles, 90095, USA

Monolithic molybdenum trioxide aerogels and xerogels have been synthesized by the sol-gel method. A three-dimensional molybdenum oxide network is achieved by suppressing Mo=O bond formation through a ligand exchange process. IR spectroscopy is used to characterize the bond formations during gelation, aging, and drying of the gels. The as-prepared aerogels are low density ($0.15\text{--}0.30\text{ g cm}^{-3}$) amorphous materials with surface areas of $150\text{--}180\text{ m}^2\text{ g}^{-1}$. Upon heating to $400\text{ }^\circ\text{C}$, the amorphous solids crystallize to orthorhombic MoO_3 .

Molybdenum oxides are of considerable interest because of their electrical, electrochemical and catalytic properties. A variety of molybdenum oxides (and molybdenum oxide hydrates) undergo reversible lithium intercalation/deintercalation reactions which are required for electrode materials in lithium batteries¹ and electrochromic devices.² The two-dimensional layered structure of orthorhombic MoO_3 has generated considerable interest as a cathode material for secondary lithium batteries, accommodating up to 1.5 Li/Mo and providing good discharge capacity ($>300\text{ mAh g}^{-1}$).³⁻⁵ The use of molybdenum oxides as catalyst materials is well established.⁶

Sol-gel chemistry is widely used to synthesize a variety of oxides based on the polymerization of molecular precursors *via* wet chemical methods.⁷ The low synthesis temperatures often lead to the formation of oxides with amorphous or metastable phases which are not produced by other synthesis routes. In some instances, the low temperature phases exhibit properties which are substantially different from the conventional phase. One example of this difference is lithium intercalation of V_2O_5 . Intercalation of orthorhombic V_2O_5 produces a series of $\text{Li}_x\text{V}_2\text{O}_5$ phases which, for $x > 1$, lose their reversibility because of the formation of the γ -phase which cannot be deintercalated.⁸ Sol-gel derived V_2O_5 exhibits a novel morphology involving one-dimensional stacking of ribbons⁹ along with substantially greater intercalation and reversibility ($4\text{ Li/V}_2\text{O}_5$) than the crystalline form.¹⁰ The sol-gel method is also valuable for synthesizing catalytic materials. In this case the use of supercritical drying methods to remove the solvent leads to the formation of high porosity, high surface area aerogels.^{11,12} The resulting aerogel catalysts exhibit unique structural and chemical properties which are not readily achievable by other preparation methods.

The sol-gel synthesis of molybdenum oxides has received relatively little attention, especially in comparison to transition metal oxides such as TiO_2 , V_2O_5 and WO_3 .⁷ The sol-gel synthesis studies reported to date have used the hydrolysis of various precursors followed by controlled heat treatments as routes to prepare powders of MoO_3 ,¹³⁻¹⁶ Mo_8O_{23} ^{14,16} and Mo_3O_5 .¹⁷ For the MoO_3 system, the reactions leading to gel formation and the nature of the intermediate xerogels were only briefly characterized. The blue color reported for the as-prepared xerogels is related to the presence of Mo^{5+} and Mo^{6+} (*i.e.*, the molybdenum blue species).¹⁸ One key feature in these sol-gel derived MoO_3 systems is the presence of well defined Mo=O peaks.¹³⁻¹⁶ Yanovskaya *et al.*¹⁵ proposed that the presence of Mo=O in all hydrolyzed alkoxide products was responsible for the formation of particulate sols and colloidal particles, rather than the branched three-dimensional

networks observed for tungsten alkoxide systems.¹⁶ This point would seem to be consistent with the observation that only the formation of xerogel and aerogel powders have been described in the literature. The only molybdenum oxide aerogels reported to date were prepared by supercritical drying (methanol solvent) of precipitates formed from molybdenum(VI) acetylacetonate (in methanol) reacted with an ammonia solution.^{19,20} Heat treatment in vacuum and hydrogen (at $430\text{ }^\circ\text{C}$) gave rise to high conductivity MoO_2 aerogels with surface areas of between 80 and $170\text{ m}^2\text{ g}^{-1}$. Catalytic activity for Ni¹⁹ and Pt²⁰ on MoO_2 aerogel powders was observed.

The present paper describes a new synthetic approach for sol-gel derived molybdenum oxides whereby the Mo=O bonds are suppressed by complexing the precursor alkoxide with nitrile ligands. Stable polymeric sols are produced leading to monolithic xerogel and aerogel samples. The as-prepared aerogels are amorphous, hydrated molybdenum oxides with low density and high surface area. The phase and hydration state of these materials are readily controlled through heat treatment.

Experimental

Synthesis method

Molybdenum trioxide aerogels were prepared using molybdenum alkoxides, acetonitrile, nitric acid and water. Two molybdenum alkoxides were used, molybdenum isopropoxide [$\text{Mo}(\text{OC}_3\text{H}_7)_5$, Alpha Aesar] and molybdenum trichloride isopropoxide [$\text{MoCl}_3(\text{OC}_3\text{H}_7)_2$, Chemat Technology], both of which were dissolved in isopropyl alcohol. The isopropyl alcohol was removed through vacuum evaporation and replaced with acetonitrile (CH_3CN , Aldrich). Nitric acid and water were then added with vigorous stirring to form the final sol. The molar ratios of acetonitrile:Mo (0:1 to 40:1) and of water:Mo (0:1 to 50:1) were varied in order to determine the composition range for gel formation.

After gelation the samples were aged in closed containers for 2-4 weeks. Longer aging times generally yielded stronger gels. In a typical preparation, gels with a molar ratio of 1:15:1:10 for the system Mo-acetonitrile-nitric acid (15.8 M)- H_2O were aged for 3 weeks. After aging, the gels were removed from their containers, immersed and then washed several times with anhydrous acetone to ensure complete replacement of water-acetonitrile with acetone. The acetone-exchanged gels were transferred to the supercritical dryer (Polaron E3000 supercritical dryer) whose chamber was cooled

to 15 °C (Forma Scientific cooling bath circulator 2006) and then filled with liquid CO₂. A minimum of four repetitive purge–fill cycles was needed to completely flush acetone from the gel. The temperature was then raised to 42 °C while increasing the pressure to 10.3 MPa. After *ca.* 15 min, the CO₂ was vented slowly. Typical samples were prepared in the form of cylinders, 1 cm in diameter by 1.5 cm in length.

To prepare xerogels, the sample containers were opened to air after the aging period. After 1 week of ambient drying, the gels were heated to 110 °C for 3 h for complete solvent removal.

Characterization

Physical properties of the aerogels and xerogels were determined using various analysis techniques. Thermogravimetry (TG, Dupont 9900 thermal analysis system) measurements were performed from 25 to 500 °C in air at a heating rate of 10 °C min⁻¹. Differential thermal analysis (TA Instruments 2910 differential scanning calorimeter base with a DTA 1600 cell) measurements were conducted in air at a heating rate of 10 °C min⁻¹. Nitrogen gas adsorption analysis (Micromeritics, ASAP 2010) was used to determine the surface area and pore size distributions of the aerogels and xerogels. In these experiments small monoliths of aerogels and xerogels were outgassed under vacuum at 180 °C for 10 h prior to the gas adsorption measurement to ensure the removal of all adsorbed water. The surface area was determined using multipoint BET analysis while the pore size distribution was determined by the BJH model. The bulk densities of the aerogels and xerogels were determined with a Hg pycnometer. The surface tension of the mercury prevents penetration of the pores when measuring mass and volume displacement of the mercury by the gels. The skeletal densities of the aerogels and xerogels were measured with a gas pycnometer (Micromeritics, AccuPyc 1330). Powder X-ray diffraction (XRD) measurements were performed on a Rigaku diffractometer in reflection mode (Cu-K α source). Transmission electron microscopy (Philips, 420T) was used to determine the structure and morphology of the molybdenum oxide aerogels. The molybdenum oxide samples subjected to different heat treatments were ground into a fine powder and sprinkled onto the copper sample grid which had a Formvar/carbon support coating (Energy Beam Sciences).

FTIR measurements (Nicolet, 510P) were used to establish the types of bonds present during different stages of sol formation and the sol–gel–aerogel transformation. Two different sample preparations were used for the dry aerogels and the wet samples (aged gels and sols). For the former, the gel samples were mixed with KCl at a mass ratio of 1:100 and ground into very fine powder. The powder mixture was then pressed into a pellet at a pressure of 150 000 psi for 3 min. For the wet samples a thin layer of the molybdenum oxide sol or aged gel was spread onto the polyethylene substrate used in disposable IR cards (3M, Type 61). The IR measurements were made from 400 to 4000 cm⁻¹. A background scan was taken for both types of sample preparations and subtracted from the IR spectra in order to account for the effect of using different preparations. Chemical composition was determined by atomic absorption and the Perkin Elmer 240C elemental analyzer (Texas Analytical Laboratories).

Results

Synthesis

Use of the two different molybdenum alkoxides [Mo(OC₃H₇)₅ and MoCl₃(OC₃H₇)₂] at a 1:1 molar ratio produced the strongest gel. The exact reason for this has not been determined but is most likely related to the presence of Cl⁻ included in one of the precursors. The samples discussed here all have a 1:1 molar ratio of the two molybdenum alkoxides. Fig. 1 shows the composition regions that formed precipitates (I),

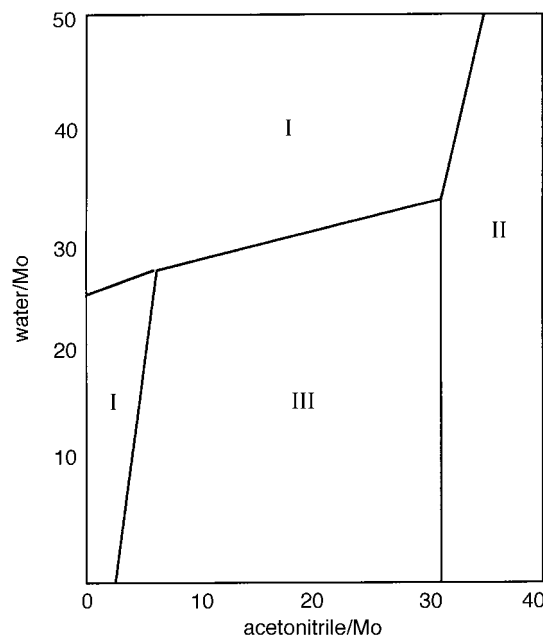


Fig. 1 Composition regions for molybdenum oxide gels. Region I, precipitates; region II, sols; region III, monolithic gels.

sols (II), and gels (III). Generally, the gelation time decreased with increased water to metal alkoxide ratio, whereas the density of the gel decreased with increased acetonitrile to water ratio. Depending on the exact composition, gelation time can range from 2 days (water to Mo ratio above 20) to 2 months (water to Mo ratio below 10). When isopropyl alcohol or acetone was used as the solvent, very rapid hydrolysis and condensation (on the order of seconds) resulted in precipitation instead of formation of a three-dimensional network.

Bulk and skeletal densities for molybdenum oxide aerogels and xerogels are listed in Table 1. The density of crystalline MoO₃ at room temperature is 4.69 g cm⁻³.¹⁸ The fact that the skeletal density of the molybdenum oxide gels is lower than the crystalline form is consistent with the amorphous structure of the as-prepared aerogels and xerogels. The bulk densities show that the aerogels are in the range of 90–95% porosity.

FTIR

FTIR has been used to characterize the chemical changes occurring during sol synthesis (Table 2) and during the sol–gel–aerogel or xerogel transformation (Table 3). The interpretation of these results is based on the IR spectra reported for MoO₃ and other molybdates.^{13–15,21–25} Because the observed IR peaks are influenced by both the bond length between Mo and O and the bond angle,²¹ various authors' reported values differ slightly in their assignments of bonds and also from those observed in the present work. Nonetheless, in the region between 500 and 1100 cm⁻¹ most of the peaks are distinct enough to allow identification.

Fig. 2 illustrates the chemical changes that occur as the metal alkoxide precursors, acetonitrile, nitric acid, and water are combined to form the final sol. Curve (e) is the spectrum of the final sol composed of the metal alkoxide precursors, acetonitrile, nitric acid, and water in the ratio of 1:15:1:10. The key features to note in the formation of the sol are the evolution of the Mo–O bonds and the absence of Mo=O bonds (1000 and 970 cm⁻¹). Four distinct molybdenum oxygen peaks are also observed in the sol. Two Mo–O–Mo vibrations of Mo⁵⁺ (957 and 750 cm⁻¹) are preserved from the non-complexed metal precursors [curves (a) and (b)].^{22–24} Two more peaks for bridging oxygen bonds are observed only after the addition of other precursors. The *cis*-O–Mo–O bond of Mo⁴⁺ (920 cm⁻¹)¹⁶ appears after the addition of

Table 1 Physical properties of molybdenum oxide aerogels and xerogels

molar ratios of Mo:CH ₃ CN:acid ^a :H ₂ O	bulk density ^b / g cm ⁻³	skeletal density ^c / g cm ⁻³	surface area ^d / m ² g ⁻¹	pore volume ^e / cm ³ g ⁻¹	av. pore diameter ^f / Å
aerogels					
1:15:1:7	0.19	3.2	160	0.60	348
1:15:1:8	0.19	3.7	179	2.92	488
1:15:1:10	0.17	3.2	175	3.48	651
1:15:1:20	0.21	3.5	148	3.20	623
xerogels					
1:15:1:8	2.02	3.1	4.5	0.014	123
1:15:1:20	1.46	3.0	5.6	0.013	83

^aHNO₃ (15.8 M). ^b±0.05 g cm⁻³. ^c±0.10 g cm⁻³. ^d±10 m² g⁻¹. ^e±0.2 cm³ g⁻¹. ^f±10 Å.

Table 2 Peak positions (cm⁻¹) for precursors and sol formation^a

(a) MoCl ₃ (OC ₃ H ₇) ₂	—	990 m	—	949 m	—	—	814 s	750 w (br)	—
(b) Mo(OC ₃ H ₇) ₅	—	—	957 s	—	—	—	814 s (sp)	—	—
(c) metal alkoxides+CH ₃ CN	1038 m (sp)	990 m	—	949 w	920 m	868 w	814 s	750 w (br)	633 w
(d) metal alkoxides+CH ₃ CN+HNO ₃	1038 m (sp)	—	957 w (br)	—	920 w (br)	868 w (br)	—	—	—
(e) final sol; curve d +H ₂ O	1038 m (sp)	—	957 m (sp)	—	920 m	868 w (br)	—	—	—

^aw = Weak, m = medium, s = strong, br = broad, sp = sharp.

Table 3 Peak positions (cm⁻¹) for different stages of the sol-gel-aerogel (xerogel) transformation^a

sol	1038 m	957 s	920 s	—	—	—	—	640 w	581 w
wet gel	—	957 m	920 s	—	868 w (br)	750 m (br)	692 m (br)	640 w	581 w
xerogel	—	957 m	920 m	900 m (br)	868 w (br)	750 m (br)	692 m (br)	640 w	581 s
aerogel	—	957 (sh)	—	900 m (br)	868 m	—	692 m (br)	640 w	581 m

^aw = Weak, m = medium, s = strong, br = broad, sh = shoulder.

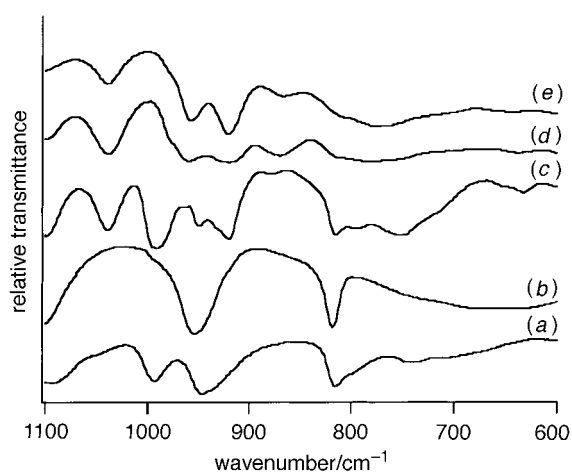


Fig. 2 FTIR spectra (600–1100 cm⁻¹) showing the formation of the molybdate sol; (a) MoCl₃(OC₃H₇)₂ (precursor), (b) Mo(OC₃H₇)₅ (precursor), (c) metal alkoxide+CH₃CN (solvent), (d) metal alkoxide+CH₃CN+HNO₃ (acid catalyst), (e) final sol

acetonitrile [curve (c)]. The change in valency (from Mo⁵⁺ to Mo⁴⁺) can be interpreted as evidence that the lone pair nitrogen is forming a bond with the metal atom. Another Mo—O—Mo absorption peak (868 cm⁻¹)²⁵ is observed after the addition of acetonitrile [curve (c)] and becomes more prominent as the final sol is formed with the addition of nitric acid and water [curves (d) and (e)]. The characteristic Mo—O stretch in the presence of Cl (990 cm⁻¹)²⁶ is present in the precursor [curve (a)] but is not observed in the final sol. Since this band diminishes after the addition of nitric acid, it suggests that the halide is no longer bound to the molybdenum. The methyl peak at 1038 cm⁻¹ is introduced from the addition of acetonitrile [curve (c)].

As the sol is aged, nitrile bonds to the Mo are replaced by oxo and hydroxy bonds, leading to a three-dimensional network and a monolithic gel. The disappearance of the nitrile

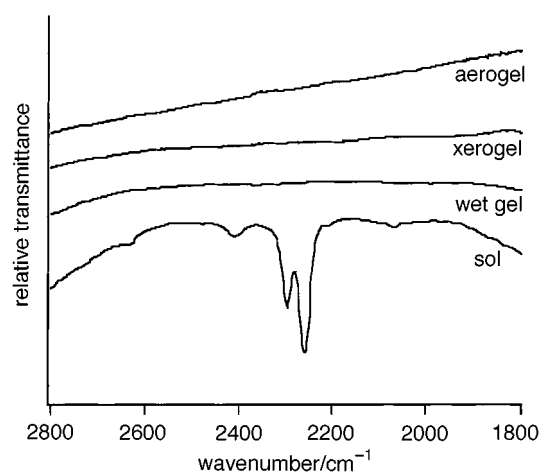


Fig. 3 FTIR spectra (1800–2800 cm⁻¹) showing the different stages of the sol-gel process for the MoO_{3-x} gel. The nitrile doublet (2295 and 2255 cm⁻¹) disappears after gelation.

doublet (2255 and 2295 cm⁻¹) is shown in Fig. 3. Fig. 4 shows the spectral changes occurring during the different stages of the sol-gel process. It is evident that bridging Mo—O bonds form during gelation and that bonds characteristic of Mo⁴⁺ and Mo⁵⁺ are gradually replaced by Mo⁶⁺ during aging and drying. In the sol, the absorption bands observed are of the methyl ligand (1038 cm⁻¹), bridging Mo—O—Mo of Mo⁴⁺ (920 and 957 cm⁻¹) and bridging Mo—O—Mo of Mo⁶⁺ (640 and 581 cm⁻¹).²⁴ Once gelation occurs (wet gel), the methyl ligand absorption band is no longer observed. Additional bridging Mo—O—Mo absorption peaks characteristic of Mo⁵⁺ (750 cm⁻¹) and Mo⁶⁺ appear (868 and 692 cm⁻¹).²⁴ As the wet gel is aged and then dried (xerogel), an additional Mo—O peak for Mo⁶⁺ emerges (900 cm⁻¹).²⁶ After the gel is supercritically dried (aerogel), the absorption bands for Mo⁴⁺ and Mo⁵⁺ diminish and the spectrum becomes more characteristic of a phase containing Mo⁵⁺ and Mo⁶⁺ than for Mo⁴⁺

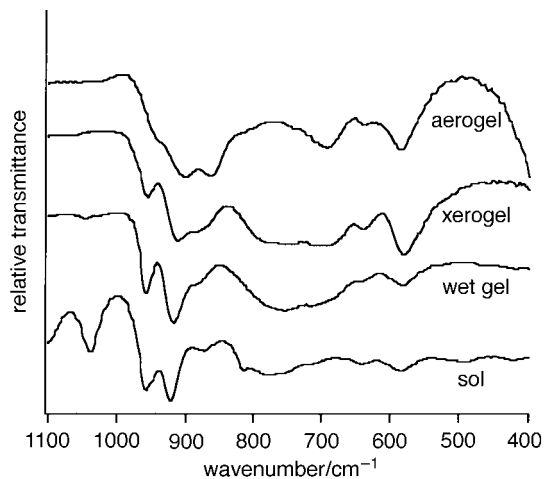


Fig. 4 FTIR spectra (400–1100 cm^{-1}) showing Mo–O bond formation during gelation, aging and drying stages

and Mo^{5+} . Because some lower valent Mo peaks still remain in the aerogel spectrum, the aerogels are most likely in the 'molybdenum blue'¹⁸ phase and not purely MoO_3 .

Physical properties

The as-prepared molybdenum oxide aerogels are amorphous and remain amorphous up to 300 °C. XRD scans (Fig. 5) exhibit no indication of broad peaks suggesting that this molybdenum oxide phase does not exhibit distinct nanocrystalline features. These materials are also amorphous in electron diffraction. The TEM micrographs show that the as-prepared aerogel has an open, branched, three-dimensional network structure with pores in the range of 100–500 Å in diameter (Fig. 6). Gas adsorption analysis of the amorphous aerogel gives a BET surface area of 150–180 $\text{m}^2 \text{g}^{-1}$ and an average pore diameter between 350–650 Å (Table 1). In contrast to the aerogels, molybdenum oxide xerogels have surface areas in the range of 5–10 $\text{m}^2 \text{g}^{-1}$ and the average pore diameter ranged between 80 and 130 Å. The molybdenum oxide aerogels and xerogels are mesoporous materials with no significant amount of micropores as can be seen from the representative pore size distributions seen in Fig. 7.

Chemical analysis and TG were used to calculate the gel compositions and show that the as-prepared molybdenum oxide aerogels are actually hydrated molybdenum oxides which contain a small amount of organics from the complexation reaction. The hydrated molybdenum oxide has a calculated

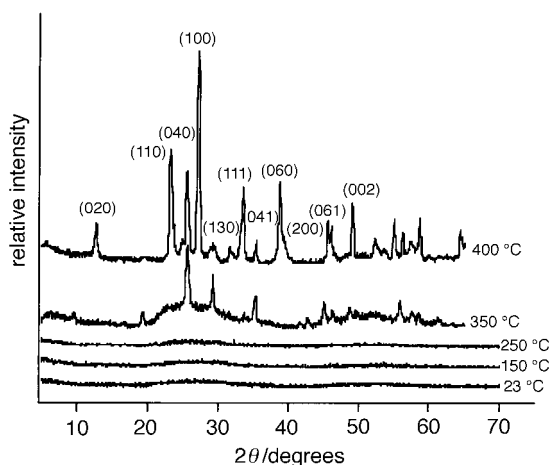


Fig. 5 X-Ray diffraction pattern of molybdenum oxide aerogels heat treated at different temperatures. Crystallization to the orthorhombic phase starts at 350 °C and is completed by 400 °C.

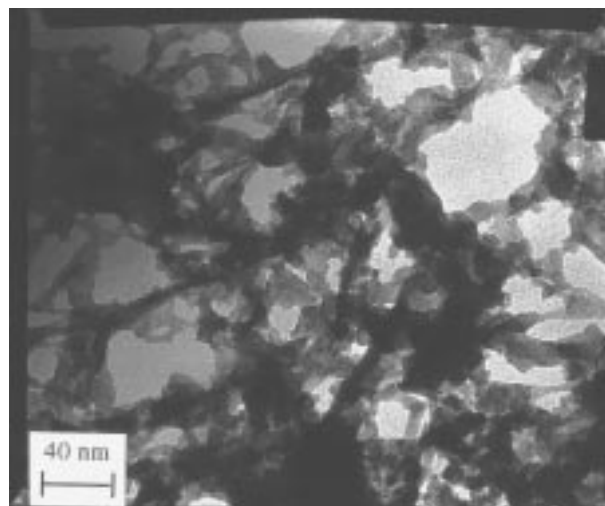


Fig. 6 TEM micrograph of the as-prepared molybdenum oxide aerogel

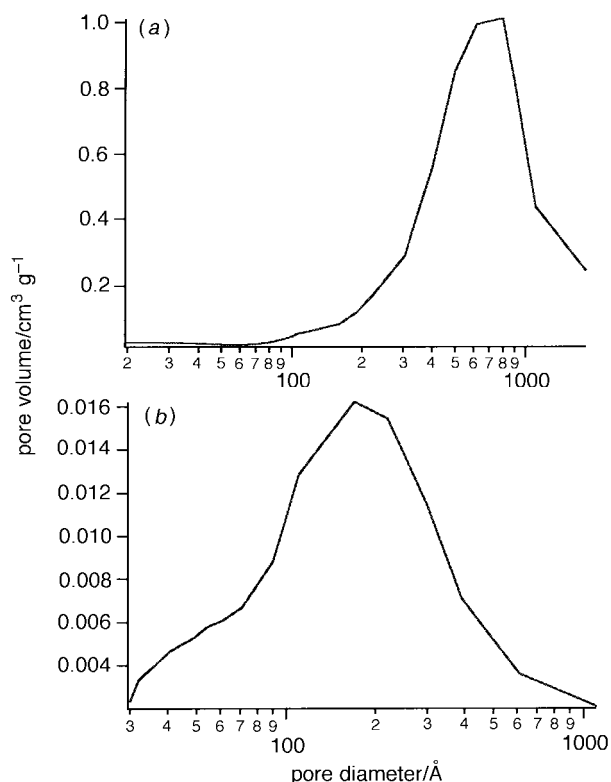


Fig. 7 BJH pore size distribution for (a) an aerogel (Mo: acetonitrile: nitric acid: H_2O at a molar ratio of 1: 15: 1: 10) and (b) a xerogel (same composition as the aerogel)

composition close to $\text{MoO}_3 \cdot 1.0\text{H}_2\text{O} \cdot 0.3\text{CH}_3\text{NH}_2$; observed and calculated components are, respectively: Mo (58.0, 56.5), C (2.1, 4.9), N (2.0, 2.4), H (1.6, 2.0) and O (34.9, 36.9%). Structural changes occur gradually as the amorphous aerogel is heated. From Fig. 8, it can be seen that a mass loss of 7.5% occurs by 150 °C. This mass loss is due to the evaporation of the CH_3NH_2 and the adsorbed water yielding the composition $\text{MoO}_3 \cdot n\text{H}_2\text{O}$ with $n=0.8$. Another, more gradual mass loss starts at 275 °C and continues until 400 °C. This mass loss is the result of the strongly bound water being released as the oxide crystallizes. The resulting white powder has a composition corresponding to MoO_3 .

A phase transformation from amorphous to orthorhombic starts at *ca.* 350 °C and is completed by 400 °C. DTA shows that an exothermic reaction occurs at *ca.* 380 °C. This corresponds well to the DTA data found in literature.^{13,27} After

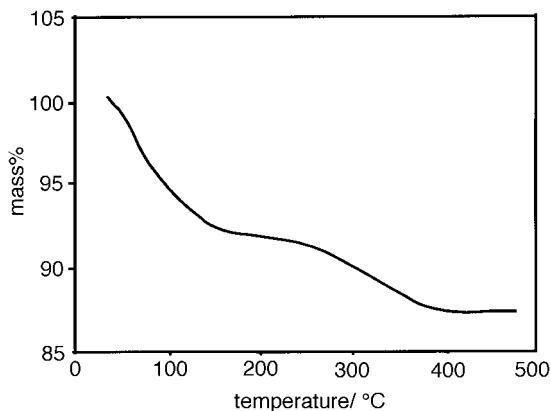


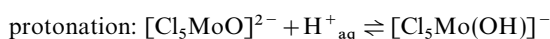
Fig. 8 Thermogravimetry for molybdenum oxide aerogel (air atmosphere; $10^{\circ}\text{C min}^{-1}$ heating rate)

heating at 400°C for 24 h, an orthorhombic phase is completely developed with $a=3.96$, $b=13.86$ and $c=3.70$ Å (Fig. 5).

Discussion

The synthesis route described here successfully suppresses formation of the terminal -yl bonds when molybdenum alkoxides are hydrolyzed. By complexing the molybdenum with nitrile bonds, hydroxy bonds that lead to bridging Mo—O—Mo bonds are more likely to form than terminal Mo=O bonds. This allows the formation of a three-dimensional network and the preparation of monolithic aerogels and xerogels which have not been reported previously.

The reason that three-dimensional networks are difficult to form with molybdenum and oxygen is that terminal bonds between molybdenum and oxygen (Mo=O) are very stable and form readily. Yanovskaya *et al.* reported that terminal oxygen atoms of molybdenum alkoxides are preserved in all hydrolysis products when $\text{MoO}_2(\text{OEt})_2$ is used.¹⁵ The terminal Mo=O, or molybdenyl, bonds are formed by sequential deprotonation of water to OH^- and finally to Mo=O. A proton transfer from a water to yl-oxygen followed by metal ion electronic rearrangement effectively exchanges the —OH to =O positions.²⁸



On the other hand, a bridging bond is formed by protonating a complex ion forming a hydroxo complex. A slowly reversible reaction would then produce a bridged oxo complex and cause isotopic exchange.²⁸



The rates of exchange for terminal and bridging oxygen bonds are very different. The bridging oxygen exchange occurs very slowly and complexation does not usually affect this exchange rate. On the other hand, the terminal or yl-oxygens exchange more rapidly and the exchange rate is very sensitive to other coordinated ligands and the solution conditions. Any ligand which replaces water in either the equatorial or apical positions will lower the rate of yl-oxygen exchange while not strongly affecting the bridging oxygen exchange rate.²⁸

In order to prevent the formation of yl-oxygen bonds, acetonitrile was used as the solvent in the sol-gel process. The original solvent for the as-received molybdenum alkoxides is isopropyl alcohol. The motivation for solvent replacement is to exchange the ligands on the molybdenum. The isopropoxide (OC_3H_7) binds to the Mo through the oxygen. This relatively weak bond can be easily replaced to form the terminating Mo=O bond once water is added. Acetonitrile is a much stronger ligand than isopropyl alcohol and will replace the

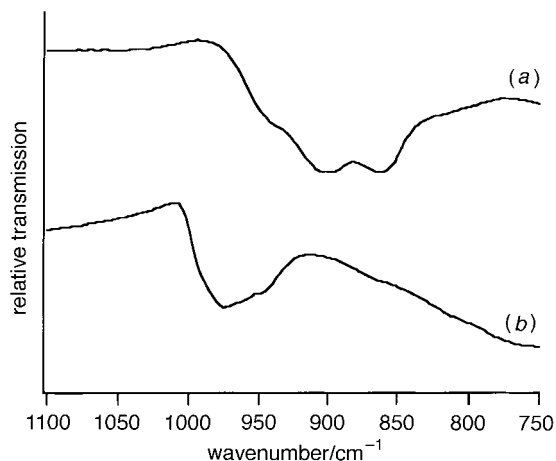


Fig. 9 IR spectra showing the presence of Mo—O—Mo and Mo=O bonds in different xerogels. (a) Spectrum of a gel that developed a three-dimensional network to form a monolithic gel and (b) spectrum of precipitates from a particulate sol that did not form a monolithic gel.

alkoxide ligands. The acetonitrile binds to Mo through the nitrogen lone pair electrons. The strongly donating CH_3CN ligands reduce the charge on the metal so that it no longer prefers the terminal oxo, which carries a -2 charge, as opposed to the bridging Mo—O—Mo bond, which has only a -1 charge.

Both Cl^- and CH_3CN ligands will lower the yl-oxygen exchange rate. Compared to Cl^- the CH_3CN ligand is much more effective owing to its large association constants and the larger number of positions occupied for a particular concentration.²⁸ Thus, by replacing the OC_3H_7 ligands with the CH_3CN ligands, the rate of hydrolysis will be slowed when water is added later. For these reasons the concentrations of acetonitrile and water are very important in determining whether a monolithic molybdenum oxide gel can be formed.

The FTIR measurements monitor the bond formations which occur during sol formation and gelation. An important feature in the FTIR data is the absence of the Mo=O absorption bands at 970 and 1000 cm^{-1} throughout the sol formation process. A spectrum of an uncomplexed gel is compared to a complexed gel (in which a three-dimensional network has formed) in Fig. 9. (It is difficult to prepare an uncomplexed sol since precipitates form immediately after the addition of water.) The peaks (901 , 860 cm^{-1}) observed for the monolithic gel [curve (a)] correspond to Mo—O—Mo bonds. These peaks are not observed for the precipitated powders [curve (b)] which, instead, exhibit a strong peak at 974 cm^{-1} representative of the Mo=O bond. These spectra are consistent with the hypothesis that in order to form a three-dimensional network and monolithic molybdenum oxide gels, the formation of the terminal oxygen bond must be suppressed.

The as-prepared molybdenum oxide aerogels and xerogels are in the form of 'molybdenum blue'. All the IR absorption bands observed in the sols and gels are indicative of molybdenum with valences lower than six; such as compounds $\text{Mo}_{13}\text{O}_{38}$, Mo_8O_{23} , $\text{Mo}_{17}\text{O}_{47}$, MoO_2 , *etc.* A true MoO_3 structure does not develop until full gelation and subsequent heat treatment. The existence of lower valent molybdenum compounds is supported by both the IR bands and the blue color of the gel. The molybdenum blue phase is composed of varying amounts of Mo^{5+} and Mo^{6+} .¹⁸

Conclusion

The synthesis approach described here uses ligand complexation to suppress Mo=O bond formation throughout the gelation and aging process of the gel. The bonds formed are bridging bonds that lead to a three-dimensional network and

the preparation of monolithic aerogels and xerogels. As-prepared aerogels are hydrated amorphous molybdenum oxides possessing low density ($0.15\text{--}0.3\text{ g cm}^{-3}$) and high surface area ($150\text{--}180\text{ m}^2\text{ g}^{-1}$). Crystallization from the amorphous to the orthorhombic phase of MoO_3 occurs between 350 and 400°C .

The authors greatly appreciate the support of this research by the Office of Naval Research.

References

- 1 G. A. Nazri and C. Julien, *Solid State Ionics*, 1994, **68**, 111.
- 2 K. Hinokuma, A. Kishimoto and T. Kudo, *J. Electrochem. Soc.*, 1994, **141**, 876.
- 3 J. P. Pereira-Ramos, N. Kumagai and N. Kumagai, *J. Power Sources*, 1995, **56**, 87.
- 4 B. Yebka and C. Julien, *Mater. Res. Soc. Symp. Proc.*, 1995, **369**, 119.
- 5 M. Sugawara, Y. Kitada and K. Matsuki, *J. Power Sources*, 1989, **26**, 373.
- 6 P. C. H. Mitchell in *Proc. First Int. Conf. on the Chemistry and Uses of Molybdenum*, ed. P. C. H. Mitchell, Climax Molybdenum Co., London, 1974, pp. 1–5.
- 7 J. Livage, M. Henry and C. Sanchez, *Prog. Solid State Chem.*, 1988, **18**, 259.
- 8 B. Pecquenard, D. Gourier and N. Baffier, *Solid State Ionics*, 1995, **78**, 287.
- 9 J. Livage, *Chem. Mater.*, 1991, **3**, 578.
- 10 A. L. Tipton, S. Passerini, B. B. Owens and W. H. Smyrl, *J. Electrochem. Soc.*, 1996, **143**, 3473.
- 11 G. M. Pajonk, *Appl. Catal.*, 1991, **72**, 217.
- 12 M. Schneider and A. Baiker, *Catal. Rev. Sci. Eng.*, 1995, **37**, 515.
- 13 J. Mendez-Vivar, A. Campero, J. Livage and C. Sanchez, *J. Non-Cryst. Solids*, 1990, **121**, 26.
- 14 J. Mendez-Vivar, *Inorg. Chim. Acta*, 1991, **179**, 77.
- 15 M. I. Yanovskaya, I. E. Obvintseva, V. G. Kessler, B. Sh. Galyamov, S. I. Kucheiko, R. R. Shifrina and N. Y. Turova, *J. Non-Cryst. Solids*, 1990, **124**, 155.
- 16 J. Mendez-Vivar, T. Lopez, A. Campero and C. Sanchez, *Langmuir*, 1991, **7**, 704.
- 17 J. A. Hollingshead, M. T. Tyszkiewicz and R. E. McCarley, *Chem. Mater.*, 1993, **5**, 1600.
- 18 D. H. Killeffer and A. Linz, *Molybdenum Compounds: Their Chemistry and Technology*, Interscience Publishers, New York, 1952.
- 19 M. Astier, A. Bertrand and S. J. Teichner, *Bull. Soc. Chim. Fr.*, 1980, **5–6**, 191.
- 20 M. Astier, A. Bertrand and S. J. Teichner, *Bull. Soc. Chim. Fr.*, 1980, **5–6**, 218.
- 21 L. Sequin, M. Figlarz, R. Cavagnat and J. C. Lassegues, *Spectrochim. Acta, Part A*, 1995, **51**, 1323.
- 22 M. Akimoto and E. Echigoya, *Chem. Lett.*, 1978, **645**, 1183.
- 23 T. Tsai, K. Maruya, M. Ai and A. Ozaki, *Bull. Chem. Soc. Jpn.*, 1982, **55**, 949.
- 24 N. Mizuno, K. Katamura, Y. Yoneda and M. Misono, *J. Catal.*, 1983, **83**, 384.
- 25 C. R. Deltcheff, R. Thouvenot and M. Fouassier, *Inorg. Chem.*, 1982, **21**, 30.
- 26 R. M. Silverstein, G. C. Bassler and T. C. Morrill, *Spectrometric Identification of Organic Compounds*, John Wiley & Sons, New York, 4th edn., 1981, p. 95.
- 27 G. A. Nazri and C. Julien, *Solid State Ionics*, 1995, **80**, 271.
- 28 G. D. Hinch, D. E. Wycoff and R. K. Murmann, *Polyhedron*, 1986, **5**, 487.

Paper 7/06537J; Received 8th September, 1997